Nanomed Res J 7(4):338-349, Autumn 2022

RESEARCH ARTICLE

Structural and morphological investigation of polycaprolactone multi-component scaffold containing collagen microsphere/ bioglass nanoparticles

Hamed Sahrapeyma[1], Azadeh Asefnejad[1*], Mahmoud Azami[2], Esmaeil Sadroddiny[3]

[1] Department of Biomedical Engineering, Science and Research Branch, Islamic Azad University, Tehran, Iran

[2] Department of Tissue Engineering, School of Advanced Technologies in Medicine, Tehran University of Medical Sciences, Tehran, Iran

[3] Medical Biotechnology Department, School of Advanced Technologies in Medicine, Tehran University of Medical Sciences, Tehran, Iran

ARTICLE INFO

Article History:
Received 01 Sep 2022
Accepted 15 Oct 2022
Published 01 Nov 2022

Keywords:
Bioglass
Polycaprolactone
Collagen microsphere
Bone tissue engineering

ABSTRACT

Bioglass nano-ceramic containing cerium (Ce) with various amounts of Ce were synthesized by sol-gel method for enhanacement polycaprolactone (PCL) fiber scaffolds for tissue engineering approaches. The prepared scaffold was analysize using scanning electron microscopy (SEM) and X-ray diffraction (XRD) to characterize the synthesized ceramic powder. The obtained results indicated proepr doping of Ce inside the bioglass microstructure. The sample were successfully encapsulated inside collagen microspheres by water-in-oil emulsion technique, an average particle size and hydrodynamic diameter of microspheres were determined by SEM images and DLS technique, respectively. The samples were submerged in the simulated body fluid (SBF) indicated that all PCL/collagen microspheres/bioglass58S/cerium fiber scaffolds have acceptable bioactivity to form apatite. In this study, the MG63 cell line cultured on PCL fiber scaffold/ collagen microspheres/bioglass 58S/cerium which indicated 3% of its potential for hard tissue approaches. The obtained results indicated that after 7 days, the rate of cell proliferation and growth increased compared to the initial days (except for PCL fiber scaffold containing collagen microspheres/bioglass 58S nanoparticles/10% cerium (mass-mass) after 7 days.

How to cite this article
Sahrapeyma H., Asefnejad A., Azami M., Sadroddiny E. Structural and morphological investigation of polycaprolactone multi-component scaffold containing collagen microsphere/bioglass nanoparticles. Nanomed Res J, 2022; 7(4): 338-349. DOI: 10.22034/nmrj.2022.04.004

INTRODUCTION

Bone tissue engineering is the most important topics in tissue engineering. Successful bone tissue replacement is highly dependent on the used scaffold properties such as biocompatibility, bioactivity, porosity, mechanical properties, and three-dimensional architecture for migration and attachment of bone cells [1-4]. Medical advances have led to increase the life expectancy of people. Bone fractures cost 17 billion $ a year in Europe and 20 billion $ in the US. Bone tissue is one of the vital and multifunctional tissues of the body known as a major component for the adult skeleton [5-8]. Bone tissue is a source of calcium, phosphate and other ions that can be stored to be effective in stabilizing the concentration of these elements in biological environment. One of the major clinical challenges in bone tissue is to repair after disease or physical injury [9-14].

The goal of tissue engineering as a field of high-tech and interdisciplinary knowledge is to repair damaged tissues and organs with modern medical tools. Therefore, one of the important

* Corresponding Author Email: *asefnejad@srbiau.ac.ir*

goals of porous bone scaffold design is to obtain an appropriate physical, biological and mechanical features [15-24]. In bone tissue engineering, three key factors are including stem cells (precursors), signals or morphogens, and scaffolds [25-29]. A porous substrate can create a suitable place to allow cell growth and proliferation. In this study, it was observed that addition of Ce may not have a negative effect on biocompatibility and formation of hydroxyapatite (HA). These elements can increase the mechanical properties by forming CeO_2 in the synthetic compound [30-39]. Therefore, PCL scaffold as a support and 3D cell culture medium, Ce and BG as an amorphous base material used for bone tissue approaches which has multiple effects on better cell attachment and proliferation. The collagen microspheres also can be useful for bone tissue approaches that using this materials confine Ce and BG as well as a substrate for the production of HA.

MATERIALS AND METHODS

In this article the synthesis of bioglass was done by sol-gel method according to the previous work [32]. Then, compounds with 1% cerium were able to form a more uniform apatite layer over a 30-day period in SBF solution according to the Kokubo protocol. Also, in Fourier transform infrared (FTIR) test indicated that the formation of these calcium phosphates (CaPs) accelerates from day 15 onwards. The purpose of this study was to prepare a scaffold with high flexibility for biological imitation of extracellular matrix (ECM) to simulate bone tissue. In this article, the aim was to prepare a 3D scaffold using PCL polymer with high elastic modulus that can create a porous substrate to allow cell growth and proliferation. The effect of Ce in BG on the repair process was also evaluated. The presence of BG mineral phase in the composition and microstructure of the scaffold can lead to the formation of CaPs and eventually HA in the scaffold. Also, the collagen layer on the surface of BG makes it possible to prevent its initial degradation in a liquid environment. Preparation of PCL scaffolds containing surface collagen microspheres can craete bone-like properties. Finally, the adhesion and growth of osteoblast cells on the scaffold were studied to evaluate the biocompatibility properties of the fabricated scaffold. Tetraethyl orthosilicate, type 1 collagen, glutaraldehyde and PCL (PCL, M_W = 80 kDa) were purchased from Sigma Aldrich (USA). Calcium nitrate tetrahydrate ($Ca(NO_3) \cdot 4H_2O$), triethyl phosphate ($C_6H_{15}O_4P$,), cerium nitrate hexahydrate ($Ce(NO_3)_3{\cdot}6H_2O$), dimethyl sulfoxide (DMSO), RPMI-1640 culture medium, phosphate buffer saline, chloroform, ethanol and methanol were purchased from Merck (Germany). Streptomycin, penicillin, bovine fetal serum and trypsin were purchased from Initrogen (Gibco, Germany). Human MG63 cell line was obtained from Pasteur Institute of Iran (Tehran, Iran). Bioglass nanopowder containing different amounts of cerium based on SiO_2–36CaO-$4P_2O_5$ (60-x) system was prepared by sol-gel method according to the previous study. In this article, for the synthesis of bioglass by sol-gel method, from tetraethyl ortho-silicate as a precursor of SiO_2, from triethyl phosphate (TEP) as a precursor of P_2O_5, from cerium nitrate hexahydrate for the supply of alkaline oxides. The required feed is used in the composition of the glass as well as the supply of cerium, deionized water twice distilled as solvent and 2M nitric acid as catalyst. Then, specific amount of water and acid were mixed with a magnetic stirrer at 400 rpm at 25°C for 20 minutes to obtain a homogeneous solvent. Then, a certain amount of tetraethyl orthosilicate was weighed and gradually added to a solution of nitric acid and distilled water and mixed on a magnetic stirrer at 400 rpm for 15 minutes at room temperature. Tetraethyl orthosilicate was initially insoluble in acid and water solvents and its droplets appeared to be suspended in the liquid, but after hydrolysis began. During this process, the reaction vessel was heated, indicating a chemical reaction. After hydrolysis of tetraethyl orthosilicate, an appropriate amount of triethyl phosphate, calcium nitrate tetrahydrate and cerium nitrate hexahydrate were added to the solution. The resulting solution was stirred for 30 minutes with a magnetic stirrer at ambient temperature to obtain a clear and homogeneous tuberculosis solution. These calculations were performed to obtain 25 g of bioglass powder containing cerium. In this synthesis method, the volume ratio of water to nitric acid is 1:6 and the molar ratio of tetraethyl ortho-silicate-triethyl phosphate solution to water is 12:1. In this study, bioglass nanoparticles containing 1, 3 and 10% cerium (mass-mass) were prepared. Cerium-free bioglass nanoparticles were also synthesized as a control sample. The resulting tuber solution was incubated at 37°C for 7 days to give a gel. For this purpose, the gel was poured into

humans and completely sealed with paraffin paper to prevent the penetration of dust by opening and closing the incubator and also to prevent the evaporation of the gel water. In the next step, the gel was dried in two steps. First, the gel was exposed to 70°C for 24 hours and the low temperature allowed the gel to dry slowly over 24 hours. The gel was then incubated at 120°C for 48 hours and to obtain a smooth and uniform powder from bioglass nanoparticles containing stabilized cerium, it was pulverized into a very soft powder by satellite milling. After complete milling and obtaining fine powder, the bioglass nanoparticle powder containing stabilized cerium was sieved to uniform size and remove large particles. For this purpose, an 8-inch steel sieve with a particle size of 37 microns. Collagen microspheres containing bioglass nanopowder with different cerium content were prepared using water-in-oil emulsion system. To do this, 1% by volume of the collagen solution was prepared by dissolving 100 mg of collagen in 10 ml of a water acetic acid solvent mixture. The volume ratio of water/acetic acid solvent mixture is 19:1 (9.5 ml of water and 0.5 ml of acetic acid), respectively. Then bioglass nanopowders containing cerium were added to the solution. The weight ratio of bioglass nanoparticles containing cerium to collagen solution is 1 to 19. Collagen solution/ bioglass/cerium using ultrasonic homogenizer (80% power, 50% -50% on-off cycle) for 5 minutes Spread evenly on the ice bath. To prepare collagen microspheres containing bioglass/cerium, 50 ml of olive oil was heated to 45°C on a magnetic stirrer at 800 RPM and 10 ml of bioglass/cerium/collagen solution was quickly sprayed into it with a syringe and the mixture was stirred for 3 hours to form an oil-in-water emulsion. To further reduce the size of the prepared microspheres, the emulsion prepared by the ultrasonic homogenizer (100% power, 70% -30% on-off cycle) was homogenized twice for 10 minutes (each time) on an ice bath. Next, to precipitate the collagen microspheres containing bioglass/cerium, the resulting solutions were placed on an ice bath at 4°C for 30 minutes to cool. Then, 40 ml of pre-cooled acetone was added to the solutions at 4°C to dehydrate and precipitate the collagen microspheres. Toluene-saturated glutaraldehyde was used to crosslink the collagen microspheres containing bioglass/cerium. For this purpose, 0.25% (w/v) of saturated glutaraldehyde in toluene was added to the solution at room temperature and incubated under laboratory hood for 18 hours. To prepare toluene-saturated glutaraldehyde, first glutaraldehyde was diluted to about 1%, then equal amounts of 1% glutaraldehyde and toluene were removed and poured into a decanter funnel and shaken gently for 10 minutes to obtain a homogeneous mixture. The above mixture was given enough time for the two phases to separate completely. The supernatant was isolated and used as a saturated glutaraldehyde in toluene. A centrifuge at 2000 rpm was used for 10 minutes to separate the cross-linked microspheres. Crosslinked microspheres were deposited on the bottom of the Falcon and collected. To remove unwanted and excess residues from the surface of the formed microspheres (separation of oil phase and glutaraldehyde residue), they were mixed twice with acetone and then centrifuged at 2000 rpm for 5 minutes. Then it was washed 3 times with distilled water and gently to remove the remaining acetone. The obtained microspheres were dried at laboratory temperature for 24 hours. Then, 400 mg of polycaprolactone (PCL) 8% (mass-volume) in 5 ml (2.5 ml of chloroform and 2.5 ml of methanol, 50:50) was added and placed on a magnetic stirrer for 24 hours to obtain a one-handed spinning solution. Collagen microspheres containing bioglass/cerium prepared in man were poured and stirred with a magnetic stirrer to evaporate the solvent (acetone). In the last step, the PCL solution was added to the microsphere collagen mixture containing bioglass/cerium and stirred on a magnetic stirrer at 100 rpm for 4 hours. Wet electrospinning of PCL scaffold containing microcirculation/cerium/bioglass nanoparticles the PCL solution containing microcirculation/ bioglass nanoparticles was poured into a 2.5 cc syringe after 24 hours of steering and placed on the injection site in a syringe pump (KDS-200, Nanoscale Technologists, Iran). Syringe pump device (uniform injection of injection solution) and voltage devices (potential difference suppliers) used for the electrospinning column (water surface supplier as collector). In this design, a single-syringe (or single nozzle) injection pump was used. Because the collector in this design was water surface and the type of electrospinning was vertical, the injection needle had to be placed on top of the electrospinning column. Therefore, a holder was placed on the spinning column to hold the injection needle, and one of the poles of the high-voltage device was attached to the tip of the needle. Due to the distance of the injection syringe inside the

syringe pump to the injection needle, the injection serum hose was used to transfer the injection solution. Also, to create the required potential difference, a metal ring was installed in the bottom of the container, which was connected to the negative pole of voltage devices. The device was a constant current potential difference (DC) with a potential difference of 0-30 kV (nanoscale technologists, Iran). This device had a potential difference resolution of 0.1 kV (100 V). To create the required potential difference, the opposite pole had to be placed in the same direction in the solution inside the electrospinning column. For this purpose, a metal ring was used which was placed in the bottom of the column and the opposite pole was connected to it through the floor hole of the device. In this design, the distance from the nozzle to the collector (in this design, the solution surface inside the electrospinning column) the syringe is placed vertically on the water/ethanol bath.

Investigation of bioactivity of prepared scaffold

After spinning the scaffold on a chloroform/methanol bath, the prepared scaffold is carefully collected and placed under a laboratory hood for 24 hours to dry. Then, for 24 hours before freezing, it was placed in the -80 freezer. Next, place the PCL/microspheric collagen/bioglass/cerium scaffold in the freezer for 72 hours to dry completely. In this study, gour types of PCL scaffolds/collagen microsphere/bioglass/containing 1, 3 and 10% cerium as experimental groups and without cerium as negative control in body simulated solution (SBF) with solid/liquid ratio of 20 mg.ml according to protocol was reviewed. The samples were soaked in SBF plastic bottles and stored at 37°C in a water bath for 7, 14 and 28 days.

Investigation of MG63 cell line binding

First, to start the study of survival coefficient and cell binding, cut the scaffold of PCL/collagen microspheres/bioglass/containing cerium with concentrations of 1, 3 and 10% (mass-mass) in the dimensions of a 24-well plate and with a sterile steel ring. It was placed at the bottom of the well. PCL/collagen microsphere/bioglass fiber scaffolds were used as negative control. According to previous research to sterilize the scaffolds, each scaffold was placed in a clean room under the UV light of a cell culture hood for 30 minutes.

Evaluation of survival coefficient on MG63 cell line

MTT colorimetric method was used to evaluate cell viability. For this purpose, MG63 cells were cultured on PCL/microfiber collagen/bioglass containing/without cerium as prepared by the above method. First, as in the mentioned protocol, the scaffolds were cut to the size of the 48-well plate and then sterilized. Sterile rims were used to hold the scaffold in the bottom of the well. After counting the cells with a neobar slide, 10^{-4} cells per well were added to the scaffold. After loading the cells, the plates were incubated in a cell culture incubator for 1, 3 and 7 days at 37°C and 5% CO_2. After 7-day of treatment, the cell culture medium was changed on the third day. At the end of the treatment period, the supernatant was discarded and the scaffold surface was gently washed with PBS to remove all excess culture medium and dead cells. Then, 20 µl of MTT solution (5 mg/ml) in PBS (pH 7.4) was added to each well and incubated for 4 hours in an incubator at 37°C and 5% CO_2.

RESULT AND DISCUSSION

The single observed peak of Bioglass 58 S sample can be related to the partial crystallization of stabilized calcium silicate under a temperature treatment of 600°C. Direct sweeping OH (Process ① in Fig. 1), and OONO− were investigated by cerium nanoparticles. In addition, previous studies have shown that cerium nanoparticles have similar effects to catalase and superoxide dismutase (SOD) (processes 1 and 2 in Fig. 1). Both effects are closely related to surface concentrations of Ce^{3+} and Ce^{4+}, pH, H_2O_2 and chelating ligand concentrations. The level of hydrophilicity of the scaffold prepared by the contact angle analysis was evaluated. As shown in Fig. 2, the hydrophilicity of the surface increases slightly with increasing cerium ion, but this increase is not significant. As shown in Fig. 2, the contact angle of the droplet with the surface in the initial second is above 100°. In the 2th second, this angle dropped below 100° (except for the control group). In the third second, the contact angle decreased again until in the fourth second, the angle decreased below 50° and the drop was absorbed by the scaffold. The MG-63 cell line is relatively immature osteoblast cells that are well-characterized and widely used for biomaterial testing, with numerous similarities to isolated human bone-derived cells. Previous research has shown that the size of the MG-63 cell line reaches more than 50 microns after 24 hours when

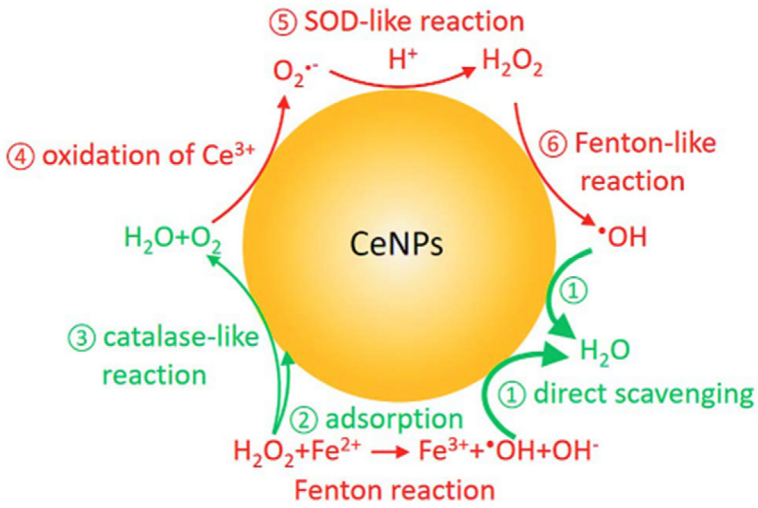

Fig. 1. Fenton reaction and reactive oxygen chemistry of cerium nanoparticles

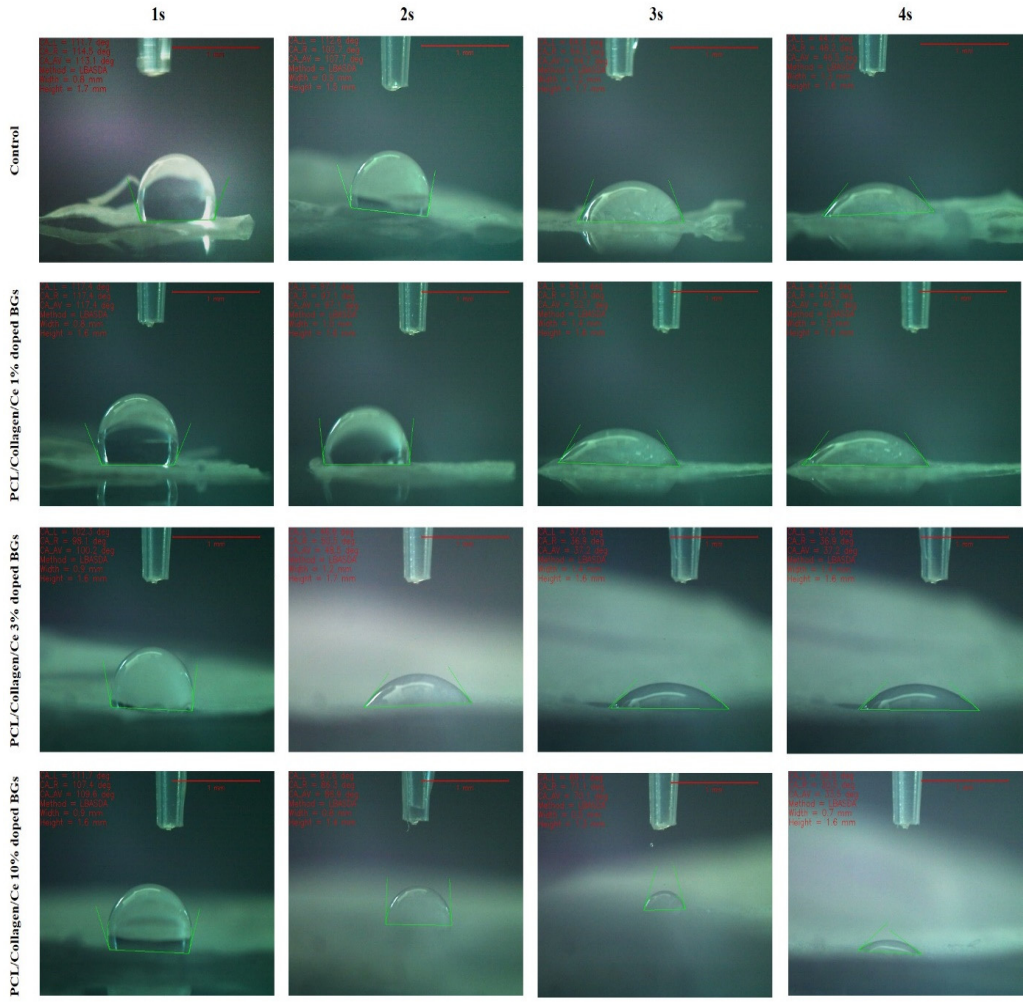

Fig. 2. Contact angle of the drop on the scaffold surface of negative control (PCL fiber scaffold), PCL fiber scaffold/1% collagen/bioglass/Ce microsphere, 1% PCL/collagen/bioglass, serum/collagen microsphere/bioglass

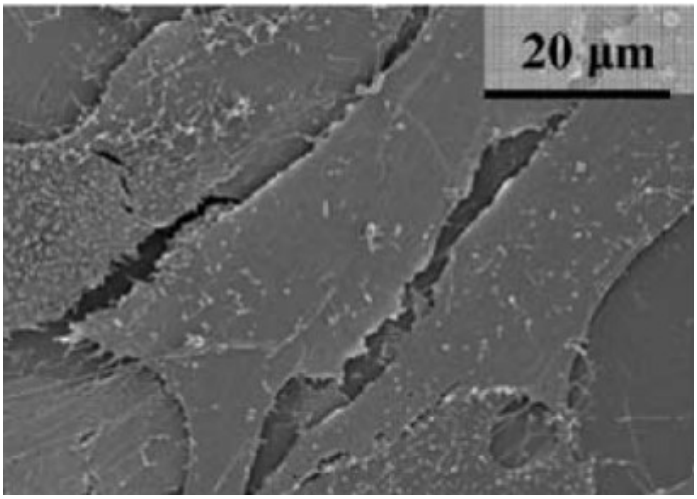

Fig. 3. SEM images of the MG-63 cell line with the morphology of MG-63 cells cultured after 24 hours

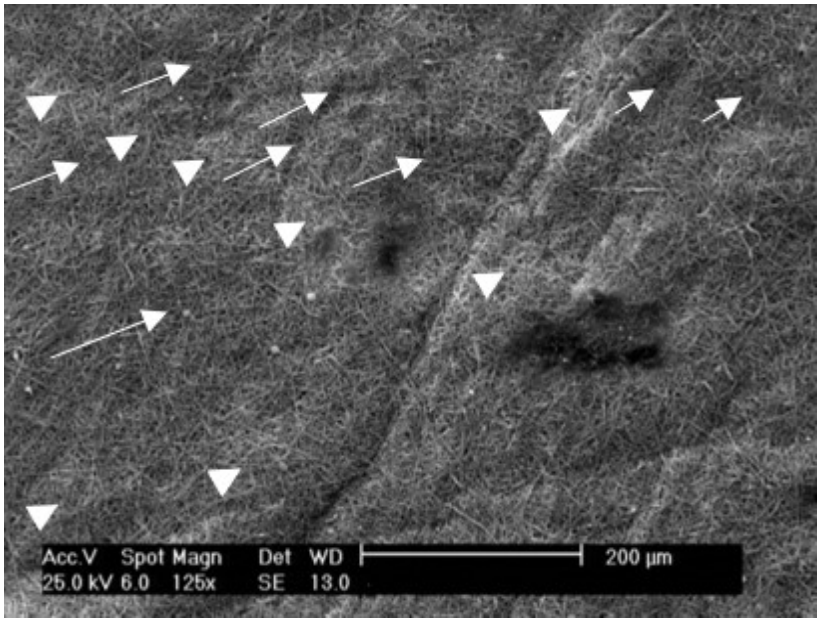

Fig. 4. SEM image of PCL fiber scaffold containing collagen microspheres/bioglass 58S nanoparticles/10% cerium after 7 days

connected to the surface. Fig. 2 indicate the cell size at 24 h after culture, which is similar to our finding, and the cell attachment to the surface of the PCL fiber scaffold containing collagen microspheres/ bioglass 58S nanoparticles/cerium 1, 3 and 10% (mass). The obtained results presented after 7 days, the rate of cell proliferation and growth increased compared to the initial days (except for PCL fiber scaffold containing collagen microspheres/bioglass 58S nanoparticles/10% cerium (mass-mass). One of the strongest probabilities about these results can be related to the high rate of cell proliferation in this sample. As can be seen it is possible that the rate of cell proliferation has reached more than 95% due to dietary and spatial limitations and possibly media acidosis. Also, the cells are exposed to food stress and pH, resulting in cell necrosis which leads to the cell density decreased. The reason can be the dark spots on the surface of the PCL fiber scaffold containing collagen microspheres/ bioglass 58S nanoparticles/10% cerium on the day 7, which have light margins. Other results confirm

the results of cytotoxicity test in which PCL fiber scaffold containing collagen microspheres/bioglass 58S nanoparticles/10% cerium (mass-mass) has a significantly higher survival rate than other samples. However, it should be noted that the number of sided cells as well as the size of the wells in the cell binding test as well as the cytotoxicity are different and the probability of cell density in the MTT test is not even close to 95%. The tensile strength of the prepared scaffolds is in accordance with Figs. 5 (a-e). Fig. 5 (a-e) shows the control sample (PCL nanofiber scaffold/collagen microsphere/BG nanoparticles) with a thickness of 0.5 mm and a scaffold ribbon width of 11.8, the maximum force tolerance was 2.7 N and the scaffold is stretched to 41.23 mm against tension. In the bioglass control sample (PCL nanofiber scaffold/bioglass nanoparticles), the scaffold with a thickness of 0.5 mm and a width of 10 mm had the highest compressive strength up to 1.5 N. The scaffold has increased in length up to 24.52 mm before tearing under pressure and it has the highest tensile strength of 0.12 N. The scaffold has increased in length up to 57.62 mm before tearing under pressure. It has the highest tensile strength of 3.1 N. The scaffold length increased up to 40.10 mm before tearing under pressure. Wet electrospinning equipment was used to create three-dimensional structures and chloroform/methanol solvent with a ratio of 1: 9 in PCL to produce thin and elongated fibers. Also, water and ethanol baths and a combination of the two were used in the collector and the formation of the resulting foam was investigated according to the porosity. It was found that the ratio of 9.1 water

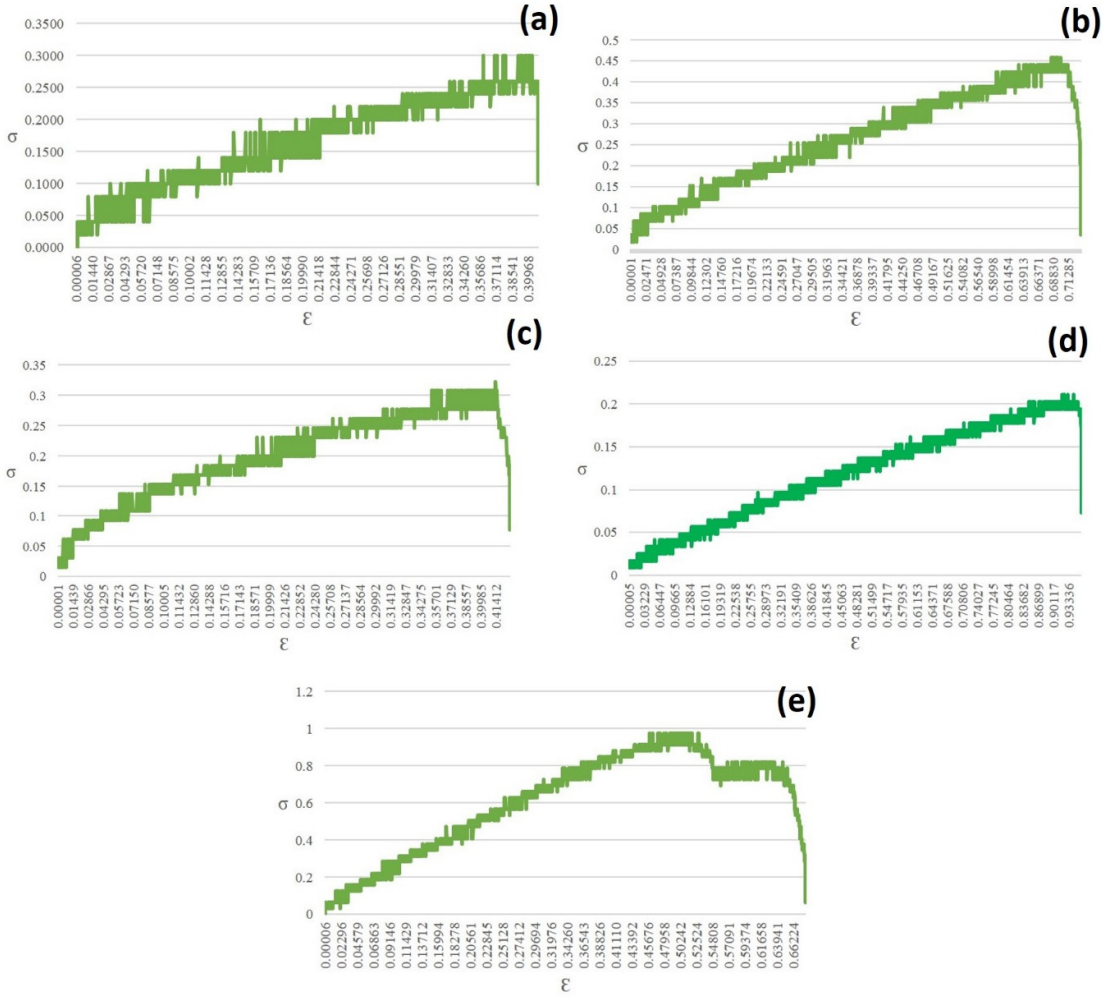

Fig. 5. Tensile strength of PCL fiber scaffolds containing collagen microspheres/bioglass 58S nanoparticles/1% cerium (mass-mass), collagen microspheres/bioglass 58S nanoparticles/1% cerium (mass-mass), containing collagen microspheres/bioglass 58S nanoparticles / 3% cerium, containing collagen microspheres/58S bioglass nanoparticles/10% cerium

and ethanol can create the best porosity in the scaffold and more uniform fibers were spun [33-44]. Researchers indicated that each of the effective parameters such as polymer concentration, solvent type, device voltage, spraying speed, needle tip to collector distance can be variable factors that can affect the size and diameter of spun fibers [45-62]. Liu et al. studied the effect of Ce on the ossification process of cells. Cerium has been shown to play an important role in osteogenesis factors and can improve ossification activity. Also, the concentration of Ce in the composition may have a direct effect on cell proliferation and alkaline phosphatase activity [3]. Calcium phosphate deposition with the presence of bioglass in the collagen scaffold was observed from the third day in the SBF test, which also precipitated hydroxyapatite particles until the 14 days. The average diameter of PCL fibers was measured at 260 nm and by loading the bioglass 58S encapsulating microspheres containing cerium inside the PCL fibers, due to the physical loading of the collagen microspheres inside the fibers, the average diameter of the PCL fibers increased to 320 ± 17 nm. Measurement of PCL scaffold fibers containing bioglass 58S encapsulating microspheres containing different concentrations of 1, 3 and 10% cerium (mass-mass) does not show any significant size difference. The average diameter of PCL fibers containing bioglass 58S encapsulated microspheres containing 3% (mass-mass) Ce concentration increased to 370 nm and also some collagen microspheres were detected on the surface of PCL nanofibers. In PCL fiber scaffolds containing bioglass 58S encapsulated microspheres containing different concentrations of 10% (mass-mass) cerium, microspheres are more detectable on the surface of the fibers and visible defects in the formation of continuous fibers due to the accumulation of microfibers in the microspheres. For example, PCL fiber scaffolds containing collagen microspheres/ bioglass 58S nanoparticles/10% cerium (mass-mass), wider band in 956 cm^{-1} compared to the sharp band of PCL fiber scaffold specimens containing microspheres of 58S 956 cm^{-1}. It has been observed that the effect of Ce nanoparticles on the crystal lattice disruption of silica groups is consistent with the SEM observations. Overlap of non-poly oxygen groups with Si-O-Si groups after seria incorporation into 58S bioglass results in the formation of a wider band in the FTIR of PCL fiber scaffold specimens containing collagen microspheres/bioglass 58S/cerium 10% in the range of 900 cm^{-1} and 1000 cm^{-1}. In the bioglass control sample, the scaffold with a thickness of 0.5 mm and a width of 10 mm had the highest compressive strength up to 1.5 N. This sample is also stretched to 24.11 mm before tearing under tensile pressure. As shown in Fig. 5, the sample is a PCL nanofiber/ collagen/bioglass/different concentrations of 1% cerium with a scaffold diameter of 5.0 mm and width 13 mm had the highest tensile strength of 2 N. The length of scaffold increased upto 24.52 mm before tearing under pressure. In the sample of PCL/microsphere collagen/bioglass nanofibers, different concentrations of 3% cerium with a scaffold diameter of 0.45 mm and a width of 13.5 mm had the highest tensile strength of 0.12 N.

Biological activity plays an important role in the development of materials for bone tissue engineering applications. To evaluate the effect of collagen microspheres/bioglass 58S nanoparticles/10% cerium enclosed in PCL fiber scaffolds, a variety of samples were prepared (PCL fiber scaffolds containing collagen microspheres/ PCL nanoparticles collagen/bioglass nanoparticles 58S/cerium 1, 3 and 10% (mass-mass)) were soaked in SBF solution for 7, 14 and 28 days. The SEM images of the samples at each time shown in Fig. 4. After 7 days of immersion of the sample in the SBF, no visible apatite formation was observed on the surface of PCL scaffold fibers containing collagen microspheres/bioglass 58S nanoparticles or PCL fiber scaffolds containing collagen microspheres/ Ce bioglass nanoparticles 58%. As can be seen, with increasing the concentration of cerium encapsulated in the microsphere within the fibers of PCL scaffolds, the crystallization rate of the phosphate group increased by about 588 cm^{-1}. It is noteworthy that the sharpest peak in the FTIR of the PCL fiber scaffold sample containing collagen microspheres/bioglass 58S nanoparticles/10% cerium (mass-mass) in the 1038 cm^{-1} region could be related to PO_4^{-3} over-formation. The porosity of the final scaffold was checked by Image-J software. The porosity was observed around 70.4%, which was a good amount for nanofiber scaffold. As shown in Fig. 2, the level of surface hydrophilicity increases slightly with increasing cerium ion, but this increase is not significant. As shown in Fig. 2, the contact angle of the droplet with the surface in the initial second above 100°. In the second second, this angle dropped below 100° (except for the control group). In the third second, in all

groups, the contact angle decreased again until in the fourth second, the angle decreased below 50° and the drop was absorbed by the scaffold. The results of this study showed that the PCL fiber scaffold sample containing collagen microspheres/ Bioglass 58S nanoparticles/10% cerium has higher biocompatibility due to its cell proliferation and higher viability at different time points. In the last decade, sodium dioxide nanoparticles have attracted much attention due to their redox properties and potential therapeutic applications. Attempts have been made to discover the potential uses of sodium dioxide as a drug. The ability of Ce-NPs to reverse the oxidation states of Ce^{3+} and Ce^{4+} makes them a suitable mediator for reactive oxygen species. Researchers worked on different nanoparticles, including bioglass and bioceramic nanoparticles, which have the ability to improve the mechanical and chemical properties of scaffolds. Also, these scaffolds were evaluated by many researchers by simulation software and suggested for dental and orthopedic applications [63-83]. The functional group OH, NO, and OONO– have been investigated by Ce-NPs. In addition, previous studies have shown that cerium nanoparticles have similar effects to catalase and superoxide dismutase (SOD). Both effects are closely related to surface concentrations of Ce^{3+} and Ce^{4+}, pH, H_2O_2 and chelating ligand concentrations. The MG-63 cell line is relatively immature osteoblast cells that are well-characterized and widely used for biomaterial testing which have many similarities to isolated human bone-derived cells.

CONCLUSION

The designed of porous scaffold is important to create a three-dimensional structure with sufficient porosity. Some parameters such as high temperature, high pH and the use of magnets in the bath can reduce the surface tension of the scaffold on water and create microstructure. In the current study, PCL fiber containing collagen microspheres-bioglass 58S nanoparticles with 1 wt%, 3 wt% and 10 wt% were successfully fabricated. The particle size of bioglass-S58 containing Ce decreases compared to bioglass, which indicates the effect of cerium on reducing the size of bioglass. The mean diameters of collagen microspheres/bioglass 58S nanoparticles and collagen microspheres/ bioglass 58S/10% cerium (mass-mass) was 340 nm and 280 nm, respectively. Biocompatibility evaluation of the prepared scaffolds indicated high cell binding and proliferation in the sample of PCL fiber scaffolds containing collagen microspheres-Bioglass 58S/3 nanoparticles (directly) and 10% (indirectly). The obtained results showed that PCL fiber scaffolds containing collagen microspheres/ Bioglass 58S nanoparticles/3% and 10% (mass-mass) can be suitable choice for repairing bone defects. Further studies should be performed in the future to evaluate the *in vivo* performance of PCL fiber scaffolds containing collagen microspheres/ Bioglass 58S nanoparticles containing 3 wt% and 10 wt% for regeneration of bone defects.

REFERENCES

1. Ismail, A. F., Othman, A., Mustafa, N. S., Kashmoola, M. A., Mustafa, B. E., & Yusof, M. Y. P. M. (2018, June). Accuracy of different dental age assessment methods to determine chronological age among Malay children. In Journal of Physics: Conference Series (Vol. 1028, No. 1, p. 012102). IOP Publishing. https://doi.org/10.1088/1742-6596/1028/1/012102
2. Yusof, M. Y. P. M., Rahman, N. L. A., Asri, A. A. A., Othman, N. I., & Mokhtar, I. W. (2017). Repeat analysis of intraoral digital imaging performed by undergraduate students using a complementary metal oxide semiconductor sensor: An institutional case study. Imaging science in dentistry, 47(4), 233-239. https://doi.org/10.5624/isd.2017.47.4.233
3. Liu, Y., Hu, Y., & Huang, L. (2014). Influence of polyethylene glycol density and surface lipid on pharmacokinetics and biodistribution of lipid-calcium-phosphate nanoparticles. Biomaterials, 35(9), 3027-3034. https://doi.org/10.1016/j.biomaterials.2013.12.022
4. Sharafabadi, A. K., Abdellahi, M., Kazemi, A., Khandan, A., & Ozada, N. (2017). A novel and economical route for synthesizing akermanite (Ca2MgSi2O7) nano-bioceramic. Materials Science and Engineering: C, 71, 1072-1078. https://doi.org/10.1016/j.msec.2016.11.021
5. Ghayour, H., Abdellahi, M., Ozada, N., Jabbrzare, S., & Khandan, A. (2017). Hyperthermia application of zinc doped nickel ferrite nanoparticles. Journal of Physics and Chemistry of Solids, 111, 464-472. https://doi.org/10.1016/j.jpcs.2017.08.018
6. Kazemi, A., Abdellahi, M., Khajeh-Sharafabadi, A., Khandan, A., & Ozada, N. (2017). Study of in vitro bioactivity and mechanical properties of diopside nano-bioceramic synthesized by a facile method using eggshell as raw material. Materials Science and Engineering: C, 71, 604-610. https://doi.org/10.1016/j.msec.2016.10.044
7. Khandan, A., Abdellahi, M., Ozada, N., & Ghayour, H. (2016). Study of the bioactivity, wettability and hardness behaviour of the bovine hydroxyapatite-diopside bio-nanocomposite coating. Journal of the Taiwan Institute of Chemical Engineers, 60, 538-546. https://doi.org/10.1016/j.jtice.2015.10.004
8. Shayan, A., Abdellahi, M., Shahmohammadian, F., Jabbarzare, S., Khandan, A., & Ghayour, H. (2017). Mechanochemically aided sintering process for the synthesis of barium ferrite: Effect of aluminum substitution on microstructure, magnetic properties and microwave absorption. Journal of Alloys and Compounds, 708, 538-546 https://doi.org/10.1016/j.jallcom.2017.02.305

9. Daud, S. M. S. M., Yusof, M. Y. P. M., Heo, C. C., Khoo, L. S., Singh, M. K. C., Mahmood, M. S., & Nawawi, H. (2022). Applications of drone in disaster management: A scoping review. Science & Justice, 62(1), 30-42. https://doi.org/10.1016/j.scijus.2021.11.002
10. Yusof, N. A. M., Noor, E., Reduwan, N. H., & Yusof, M. Y. P. M. (2021). Diagnostic accuracy of periapical radiograph, cone beam computed tomography, and intrasurgical linear measurement techniques for assessing furcation defects: a longitudinal randomised controlled trial. Clinical oral investigations, 25(3), 923-932. https://doi.org/10.1007/s00784-020-03380-8
11. Yusof, N. A. M., Noor, N., & Yusof, M. Y. P. M. (2019). The accuracy of linear measurements in cone beam computed tomography for assessing intrabony and furcation defects: A systematic review and meta-analysis. Journal of Oral Research, 8(6), 527-539. https://doi.org/10.17126/joralres.2019.077
12. Angelakopoulos, N., Galić, I., Balla, S. B., Kiş, H. C., Gómez Jiménez, L., Zolotenkova, G., ... & Cameriere, R. (2021). Comparison of the third molar maturity index (I3M) between left and right lower third molars to assess the age of majority: A multi-ethnic study sample. International journal of legal medicine, 135(6), 2423-2436. https://doi.org/10.1007/s00414-021-02656-2
13. Adam, F. A., Mohd, N., Rani, H., Baharin, B., & Yusof, M. Y. P. M. (2021). Salvadora persica L. chewing stick and standard toothbrush as anti-plaque and anti-gingivitis tool: A systematic review and meta-analysis. Journal of ethnopharmacology, 274, 113882. https://doi.org/10.1016/j.jep.2021.113882
14. Mohammad, N., Muad, A. M., Ahmad, R., & Yusof, M. Y. P. M. (2021). Reclassification of Demirjian's mandibular premolars staging for age estimation based on semi-automated segmentation of deep convolutional neural network. Forensic Imaging, 24, 200440. https://doi.org/10.1016/j.fri.2021.200440
15. Yusof, M. Y. P. M., Mah, M. C., Reduwan, N. H., Kretapirom, K., & Affendi, N. H. K. (2020). Quantitative and qualitative assessments of intraosseous neurovascular canals in dentate and posteriorly edentulous individuals in lateral maxillary sinus wall. The Saudi dental journal, 32(8), 396-402. https://doi.org/10.1016/j.sdentj.2019.10.010
16. Mohammad, N., Yusof, M. Y. P. M., Ahmad, R., & Muad, A. M. (2020, March). Region-based segmentation and classification of Mandibular First Molar Tooth based on Demirjian's method. In Journal of Physics: Conference Series (Vol. 1502, No. 1, p. 012046). IOP Publishing. https://doi.org/10.1088/1742-6596/1502/1/012046
17. Khandan, A., Abdellahi, M., Ozada, N., & Ghayour, H. (2016). Study of the bioactivity, wettability and hardness behaviour of the bovine hydroxyapatite-diopside bio-nanocomposite coating. Journal of the Taiwan Institute of Chemical Engineers, 60, 538-546. https://doi.org/10.1016/j.jtice.2015.10.004
18. Karamian, E., Motamedi, M. R. K., Khandan, A., Soltani, P., & Maghsoudi, S. (2014). An in vitro evaluation of novel NHA/zircon plasma coating on 316L stainless steel dental implant. Progress in Natural Science: Materials International, 24(2), 150-156. https://doi.org/10.1016/j.pnsc.2014.04.001
19. Karamian, E., Abdellahi, M., Khandan, A., & Abdellah, S. (2016). Introducing the fluorine doped natural hydroxyapatite-titania nanobiocomposite ceramic. Journal of Alloys and Compounds, 679, 375-383. https://doi.org/10.1016/j.jallcom.2016.04.068
20. Najafinezhad, A., Abdellahi, M., Ghayour, H., Soheily, A., Chami, A., & Khandan, A. (2017). A comparative study on the synthesis mechanism, bioactivity and mechanical properties of three silicate bioceramics. Materials Science and Engineering: C, 72, 259-267. https://doi.org/10.1016/j.msec.2016.11.084
21. Khandan, A., & Ozada, N. (2017). Bredigite-Magnetite (Ca7MgSi4O16-Fe3O4) nanoparticles: A study on their magnetic properties. Journal of Alloys and Compo https://doi.org/10.1016/j.jallcom.2017.07.288
22. Al-Harbi, N., Mohammed, H., Al-Hadeethi, Y., Bakry, A. S., Umar, A., Hussein, M. A., ... & Nune, M. (2021). Silica-based bioactive glasses and their applications in hard tissue regeneration: A review. Pharmaceuticals, 14(2), 75. https://doi.org/10.3390/ph14020075
23. Heydary, H. A., Karamian, E., Poorazizi, E., Khandan, A., & Heydaripour, J. (2015). A novel nano-fiber of Iranian gum tragacanth-polyvinyl alcohol/nanoclay composite for wound healing applications. Procedia Materials Science, 11, 176-182. https://doi.org/10.1016/j.mspro.2015.11.079
24. Shahgholi, M., Oliviero, S., Baino, F., Vitale-Brovarone, C., Gastaldi, D., & Vena, P. (2016). Mechanical characterization of glass-ceramic scaffolds at multiple characteristic lengths through nanoindentation. Journal of the European Ceramic Society, 36(9), 2403-2409. https://doi.org/10.1016/j.jeurceramsoc.2016.01.042
25. Fada, R., Farhadi Babadi, N., Azimi, R., Karimian, M., & Shahgholi, M. (2021). Mechanical properties improvement and bone regeneration of calcium phosphate bone cement, Polymethyl methacrylate and glass ionomer. Journal of Nanoanalysis, 8(1), 60-79.
26. Jabbarzare, S., Abdellahi, M., Ghayour, H., Arpanahi, A., & Khandan, A. (2017). A study on the synthesis and magnetic properties of the cerium ferrite ceramic. Journal of Alloys and Compounds, 694, 800-807. https://doi.org/10.1016/j.jallcom.2016.10.064
27. Razavi, M., & Khandan, A. (2017). Safety, regulatory issues, long-term biotoxicity, and the processing environment. In Nanobiomaterials Science, Development and Evaluation (pp. 261-279). Woodhead Publishing. https://doi.org/10.1016/B978-0-08-100963-5.00014-8
28. Bagher, Z., Ehterami, A., Safdel, M. H., Khastar, H., Semiari, H., Asefnejad, A., ... & Salehi, M. (2020). Wound healing with alginate/chitosan hydrogel containing hesperidin in rat model. Journal of Drug Delivery Science and Technology, 55, 101379. https://doi.org/10.1016/j.jddst.2019.101379
29. Asefnejad, A., Khorasani, M. T., Behnamghader, A., Farsadzadeh, B., & Bonakdar, S. (2011). Manufacturing of biodegradable polyurethane scaffolds based on polycaprolactone using a phase separation method: physical properties and in vitro assay. International journal of nanomedicine, 6, 2375. https://doi.org/10.2147/IJN.S15586
30. Abasalta, M., Asefnejad, A., Khorasani, M. T., & Saadatabadi, A. R. (2021). Fabrication of carboxymethyl chitosan/poly (ε-caprolactone)/doxorubicin/nickel ferrite core-shell fibers for controlled release of doxorubicin against breast cancer. Carbohydrate Polymers, 257, 117631. https://doi.org/10.1016/j.carbpol.2021.117631
31. Saeedi, M., Abdellahi, M., Rahimi, A., & Khandan, A. (2016). Preparation and characterization of nanocrystalline barium ferrite ceramic. Functional Materials Letters, 9(05), 1650068. https://doi.org/10.1142/S1793604716500685
32. Sahrapeyma, H., Asefnejad, A., Azami, M., & Sadroddiny, E. (2021). Fabrication of fibrous poly (ε-caprolactone) nano-fibers containing cerium doped-bioglasses nanoparticles encapsulated collagen. Journal

of Applied Polymer Science, 138(41), 51202. https://doi.org/10.1002/app.51202
33. Khandan, A., Ozada, N., & Karamian, E. (2015). Novel microstructure mechanical activated nano composites for tissue engineering applications. J Bioeng Biomed Sci, 5(1), 1.
34. Ghayour, H., Abdellahi, M., Bahmanpour, M., & Khandan, A. (2016). Simulation of dielectric behavior in RFeO $$ _ {3} $$3 orthoferrite ceramics (R= rare earth metals). Journal of Computational Electronics, 15(4), 1275-1283. https://doi.org/10.1007/s10825-016-0886-2
35. Khandan, A., Karamian, E., Faghih, M., & Bataille, A. (2014). Formation of AlN Nano Particles Precipitated in St-14 Low Carbon Steel by Micro and Nanoscopic Observations. Journal of Iron and Steel Research International, 21(9), 886-890. https://doi.org/10.1016/S1006-706X(14)60157-6
36. Karamian, E. B., Motamedi, M. R., Mirmohammadi, K., Soltani, P. A., & Khandan, A. M. (2014). Correlation between crystallographic parameters and biodegradation rate of natural hydroxyapatite in physiological solutions. Indian J Sci Res, 4(3), 092-9. https://doi.org/10.1155/2014/410627
37. Khandan, A., & Esmaeili, S. (2019). Fabrication of polycaprolactone and polylactic acid shapeless scaffolds via fused deposition modelling technology. Journal of Advanced Materials and Processing, 7(4), 16-29.
38. Mirzadeh, S., Asefnejad, A., Khonakdar, H. A., & Jafari, S. H. (2021). Improved surface properties in spray-coated PU/TiO2/graphene hybrid nanocomposites through nonsolvent-induced phase separation. Surface and Coatings Technology, 405, 126507. https://doi.org/10.1016/j.surfcoat.2020.126507
39. Sotoudeh, A., Darbemamieh, G., Goodarzi, V., Shojaei, S., & Asefnejad, A. (2021). Tissue engineering needs new biomaterials: Poly (xylitol-dodecanedioic acid)-co-polylactic acid (PXDDA-co-PLA) and its nanocomposites. European Polymer Journal, 152, 110469 https://doi.org/10.1016/j.eurpolymj.2021.110469
40. Mohammad, N., Yusof, M. Y. P. M., Ahmad, R., & Muad, A. M. (2020, March). Region-based segmentation and classification of Mandibular First Molar Tooth based on Demirjian's method. In Journal of Physics: Conference Series (Vol. 1502, No. 1, p. 012046). IOP Publishing. https://doi.org/10.1088/1742-6596/1502/1/012046
41. Ravi, G. R., & Subramanyam, R. V. (2012). Calcium hydroxide-induced resorption of deciduous teeth: A possible explanation. Dental Hypotheses, 3(3), 90. https://doi.org/10.4103/2155-8213.103910
42. Khandan, A., Karamian, E., & Bonakdarchian, M. (2014). Mechanochemical synthesis evaluation of nanocrystalline bone-derived bioceramic powder using for bone tissue engineering. Dental Hypotheses, 5(4), 155. https://doi.org/10.4103/2155-8213.140606
43. Karamian, E., Khandan, A., Kalantar Motamedi, M. R., & Mirmohammadi, H. (2014). Surface characteristics and bioactivity of a novel natural HA/zircon nanocomposite coated on dental implants. BioMed research international, 2014. https://doi.org/10.1155/2014/410627
44. Anttonen, V., Tanner, T., Kämppi, A., Päkkilä, J., Tjäderhane, L., & Patinen, P. (2012). A methodological pilot study on oral health of young, healthy males. Dental Hypotheses, 3(3), 106. https://doi.org/10.4103/2155-8213.103928
45. Khandan, A., Jazayeri, H., Fahmy, M. D., & Razavi, M. (2017). Hydrogels: Types, structure, properties, and applications. Biomat Tiss Eng, 4(27), 143-69. https://doi.org/10.2174/9781681085364117040007
46. Gupta, R., Thakur, N., Thakur, S., Gupta, B., & Gupta, M. (2013). Talon cusp: a case report with management guidelines for practicing dentists. Dental Hypotheses, 4(2), 67. https://doi.org/10.4103/2155-8213.113020
47. Kjaer, I. (2013). External root resorption: Different etiologies explained from the composition of the human root-close periodontal membrane. Dental Hypotheses, 4(3), 75. https://doi.org/10.4103/2155-8213.116327
48. Motamedi, M. R. K., Behzadi, A., Khodadad, N., Zadeh, A. K., & Nilchian, F. (2014). Oral health and quality of life in children: a cross-sectional study. Dental Hypotheses, 5(2), 53. https://doi.org/10.4103/2155-8213.133426
49. Narayanan, N., & Thangavelu, L. (2015). Salvia officinalis in dentistry. Dental Hypotheses, 6(1), 27. https://doi.org/10.4103/2155-8213.150870
50. Khandan, A., Karamian, E., & Bonakdarchian, M. (2014). Mechanochemical synthesis evaluation of nanocrystalline bone-derived bioceramic powder using for bone tissue engineering. Dental Hypotheses, 5(4), 155. https://doi.org/10.4103/2155-8213.140606
51. Monfared, R. M., Ayatollahi, M. R., & Isfahani, R. B. (2018). Synergistic effects of hybrid MWCNT/nanosilica on the tensile and tribological properties of woven carbon fabric epoxy composites. Theoretical and Applied Fracture Mechanics, 96, 272-284. https://doi.org/10.1016/j.tafmec.2018.05.007
52. Kamarian, S., Bodaghi, M., Isfahani, R. B., & Song, J. I. (2021). Thermal buckling analysis of sandwich plates with soft core and CNT-Reinforced composite face sheets. Journal of Sandwich Structures & Materials, 23(8), 3606-3644. https://doi.org/10.1177/1099636220935557
53. Kamarian, S., Bodaghi, M., Isfahani, R. B., & Song, J. I. (2022). A comparison between the effects of shape memory alloys and carbon nanotubes on the thermal buckling of laminated composite beams. Mechanics Based Design of Structures and Machines, 50(7), 2250-2273. https://doi.org/10.1080/15397734.2020.1776131
54. Barbaz-I, R. (2014). Experimental determining of the elastic modulus and strength of composites reinforced with two nanoparticles (Doctoral dissertation, Doctoral dissertation, MSc Thesis, School of Mechanical Engineering Iran University of Science and Technology, Tehran, Iran).
55. Mahjoory, M., Shahgholi, M., & Karimipour, A. (2022). The effects of initial temperature and pressure on the mechanical properties of reinforced calcium phosphate cement with magnesium nanoparticles: A molecular dynamics approach. International Communications in Heat and Mass Transfer, 135, 106067. https://doi.org/10.1016/j.icheatmasstransfer.2022.106067
56. Talebi, M., Abbasi-Rad, S., Malekzadeh, M., Shahgholi, M., Ardakani, A. A., Foudeh, K., & Rad, H. S. (2021). Cortical bone mechanical assessment via free water relaxometry at 3 T. Journal of Magnetic Resonance Imaging, 54(6), 1744-1751. https://doi.org/10.1002/jmri.27765
57. M. Shahgholi, P. Firouzi, O. Malekahmadi, S. Vakili, A. Karimipour, M. Ghashang, W. Hussain, Hawraa A. Kareem, S. Baghaei, Fabrication and characterization of nanocrystalline hydroxyapatite reinforced with silica-magnetite nanoparticles with proper thermal conductivity, Materials Chemistry and Physics, 2022. https://doi.org/10.1016/j.matchemphys.2022.126439
58. R. Lucchini, D. Carnelli, D. Gastaldi, M. Shahgholi, R. Contro, P. Vena, A damage model to simulate nanoindentation tests of lamellar bone at multiple penetration depth, in: ECCOMAS 2012 - European Congress on Computational Methods in Applied Sciences and Engineering, E-Book Full Papers, 2012, pp. 5919-5924.
59. Saeedi, M. R., Morovvati, M. R., & Mollaei-Dariani, B. (2020). Experimental and numerical investigation of

impact resistance of aluminum-copper cladded sheets using an energy-based damage model. Journal of the Brazilian Society of Mechanical Sciences and Engineering, 42(6), 1-24. https://doi.org/10.1007/s40430-020-02397-0
60. Kardan-Halvaei, M., Morovvati, M. R., & Mollaei-Dariani, B. (2020). Crystal plasticity finite element simulation and experimental investigation of the micro-upsetting process of OFHC copper. Journal of Micromechanics and Microengineering, 30(7), 075005. https://doi.org/10.1088/1361-6439/ab8549
61. Fazlollahi, M., Morovvati, M. R., & Mollaei Dariani, B. (2019). Theoretical, numerical and experimental investigation of hydro-mechanical deep drawing of steel/polymer/steel sandwich sheets. Proceedings of the Institution of Mechanical Engineers, Part B: Journal of Engineering Manufacture, 233(5), 1529-1546. https://doi.org/10.1177/0954405418780173
62. Saeedi, M. R., Morovvati, M. R., & Alizadeh-Vaghasloo, Y. (2018). Experimental and numerical study of mode-I and mixed-mode fracture of ductile U-notched functionally graded materials. International Journal of Mechanical Sciences, 144, 324-340. https://doi.org/10.1016/j.ijmecsci.2018.06.008
63. Morovvati, M. R., & Mollaei-Dariani, B. (2018). The formability investigation of CNT-reinforced aluminum nano-composite sheets manufactured by accumulative roll bonding. The International Journal of Advanced Manufacturing Technology, 95(9), 3523-3533. https://doi.org/10.1007/s00170-017-1205-1
64. Morovvati, M. R., & Dariani, B. M. (2017). The effect of annealing on the formability of aluminum 1200 after accumulative roll bonding. Journal of Manufacturing Processes, 30, 241-254. https://doi.org/10.1016/j.jmapro.2017.09.013
65. Morovvati, M. R., Lalehpour, A., & Esmaeilzare, A. (2016). Effect of nano/micro B4C and SiC particles on fracture properties of aluminum 7075 particulate composites under chevron-notch plane strain fracture toughness test. Materials Research Express, 3(12), 125026. https://doi.org/10.1088/2053-1591/3/12/125026
66. Fatemi, A., Morovvati, M. R., & Biglari, F. R. (2013). The effect of tube material, microstructure, and heat treatment on process responses of tube hydroforming without axial force. The International Journal of Advanced Manufacturing Technology, 68(1), 263-276. https://doi.org/10.1007/s00170-013-4727-1
67. Pourmoghadam, M. N., Esfahani, R. S., Morovvati, M. R., & Rizi, B. N. (2013). Bifurcation analysis of plastic wrinkling formation for anisotropic laminated sheets (AA2024-Polyamide-AA2024). Computational materials science, 77, 35-43. https://doi.org/10.1016/j.commatsci.2013.03.037
68. Morovvati, M. R., Fatemi, A., & Sadighi, M. (2011). Experimental and finite element investigation on wrinkling of circular single layer and two-layer sheet metals in deep drawing process. The International Journal of Advanced Manufacturing Technology, 54(1), 113-121. https://doi.org/10.1007/s00170-010-2931-9
69. Morovvati, M. R., Mollaei-Dariani, B., & Haddadzadeh, M. (2010). Initial blank optimization in multilayer deep drawing process using GONNS. Journal of manufacturing science and engineering, 132(6). https://doi.org/10.1115/1.4003121
70. Fatemi, A., Biglari, F., & Morovvati, M. R. (2010). Influences of inner pressure and tube thickness on process responses of hydroforming copper tubes without axial force. Proceedings of the Institution of Mechanical Engineers, Part B: Journal of Engineering Manufacture, 224(12), 1866-1878. https://doi.org/10.1243/09544054JEM2001
71. Anarestani, S. S., Morovvati, M. R., & Vaghasloo, Y. A. (2015). Influence of anisotropy and lubrication on wrinkling of circular plates using bifurcation theory. International Journal of Material Forming, 8(3), 439-454. https://doi.org/10.1007/s12289-014-1187-6
72. Abedpour, M., Kamyab Moghadas, B., & Tamjidi, S. (2020). Equilibrium and kinetic study of simultaneous removal of Cd (II) and Ni (II) by acrylamide-based polymer as effective adsorbent: optimisation by response surface methodology (RSM). International Journal of Environmental Analytical Chemistry, 1-18 https://doi.org/10.1080/03067319.2020.1772768
73. Tamjidi, S., Esmaeili, H., & Moghadas, B. K. (2021). Performance of functionalized magnetic nanocatalysts and feedstocks on biodiesel production: a review study. Journal of Cleaner Production, 305, 127200. https://doi.org/10.1016/j.jclepro.2021.127200
74. Ghasemi, M., Nejad, M. G., Alsaadi, N., Abdel-Jaber, M. T., Yajid, A., Shukri, M., & Habib, M. (2022). Performance measurment and lead-time reduction in epc project-based organizations: a mathematical modeling approach. Mathematical Problems in Engineering, 2022. https://doi.org/10.1155/2022/5767356
75. Davani, P. P., Kloub, A. W. M., & Ghadiri Nejad, M. (2020). Optimizing the first type of U-shaped assembly line balancing problems. Annals of Optimization Theory and Practice, 3(4), 65-82.
76. Golabi, M., & Nejad, M. G. (2022). Intelligent and fuzzy UAV transportation applications in aviation 4.0. In Intelligent and Fuzzy Techniques in Aviation 4.0 (pp. 431-458). Springer, Cham. https://doi.org/10.1007/978-3-030-75067-1_19
77. Mirzaei, N., Nejad, M. G., & Fernandes, N. O. (2021). Combining Line Balancing Methods and Discrete Event Simulation: A Case Study from a Metalworking Company. International Journal of Industrial Engineering and Management, 12(1), 14. https://doi.org/10.24867/IJIEM-2021-1-273
78. Vizvári, B., Guden, H., & G Nejad, M. (2018). Local search based meta-heuristic algorithms for optimizing the cyclic flexible manufacturing cell problem. Annals of Optimization Theory and Practice, 1(3 & 4), 15-32.
79. Ghadiri Nejad, M., & Banar, M. (2018). Emergency response time minimization by incorporating ground and aerial transportation. Annals of Optimization Theory and Practice, 1(1), 43-57.
80. Haghayegh, M., Zabihi, F., Eikani, M. H., Kamya Moghadas, B., & Vaziri Yazdi, S. A. (2015). Supercritical fluid extraction of flavonoids and terpenoids from herbal compounds: Experiments and mathematical modeling. Journal of Essential oil Bearing plants, 18(5), 1253-1265. https://doi.org/10.1080/0972060X.2014.961037
81. Moghadas, B. K., Safekordi, A. A., Honarvar, B., Kaljahi, J. F., & Yazdi, S. A. V. (2012). Experimental Study of Dorema aucheri Extraction with Supercritical Carbon Dioxide. Asian Journal of Chemistry, 24(8).
82. Mirzapour, P., Kamyab Moghadas, B., Tamjidi, S., & Esmaeili, H. (2021). Activated carbon/bentonite/Fe3O4 nanocomposite for treatment of wastewater containing Reactive Red 198. Separation Science and Technology, 56(16), 2693-2707. https://doi.org/10.1080/01496395.2020.1843051
83. Wu, J., Ling, C., Ge, A., Jiang, W., Baghaei, S., & Kolooshani, A. (2022). Investigating the performance of tricalcium phosphate bioceramic reinforced with titanium nanoparticles in friction stir welding for coating of orthopedic prostheses application. Journal of Materials Research and Technology. https://doi.org/10.1016/j.jmrt.2022.07.102